

ORIGINAL ARTICLE

The glutathione synthesis inhibitor buthionine sulfoximine synergistically enhanced melphalan activity against preclinical models of multiple myeloma

A Tagde^{1,2}, H Singh^{1,3}, MH Kang^{1,2,3} and CP Reynolds^{1,2,3,4,5}

Melphalan (L-PAM) has been an integral part of multiple myeloma (MM) treatment as a conditioning regimen before stem cell transplant (SCT). After initial response, most treated patients experience relapse with an aggressive phenotype. Increased glutathione (GSH) in MM may mediate resistance to L-PAM. We demonstrated that the GSH synthesis inhibitor buthionine sulfoximine (BSO) synergistically enhanced L-PAM activity (inducing 2–4 logs of cell kill) against nine MM cell lines (also in the presence of marrow stroma or cytokines) and in seven primary MM samples (combination indices < 1.0). In MM cell lines, BSO significantly ($P < 0.05$) depleted GSH, increased L-PAM-induced single-strand DNA breaks, mitochondrial depolarization, caspase cleavage and apoptosis. L-PAM depleted GSH, but GSH rapidly recovered in a L-PAM-resistant MM cell line unless also treated with BSO. Treatment with *N*-acetylcysteine antagonized BSO + L-PAM cytotoxicity without increasing GSH. In human MM xenografted into *beige-nude-xid* mice, BSO significantly depleted MM intracellular GSH and significantly increased apoptosis compared with L-PAM alone. BSO + L-PAM achieved complete responses (CRs) in three MM xenograft models including maintained CRs > 100 days, and significantly increased the median event-free survival relative to L-PAM alone. Combining BSO with L-PAM warrants clinical testing in advanced MM.

Blood Cancer Journal (2014) 4, e229; doi:10.1038/bcj.2014.45; published online 18 July 2014

INTRODUCTION

Multiple myeloma (MM) is a plasma cell malignancy that accounts for 63 000 annual deaths worldwide.^{1–3} Treatment regimens containing high-dose melphalan (L-PAM) supported by stem cell transplant (SCT) increased response rates and progression-free survival compared with conventional therapy.^{2,4} Despite introducing new agents and strategies, many patients eventually relapse or become refractory to current therapy.^{1,5–7} Each successive regimen achieves a less durable response, suggesting emergence of a resistant phenotype and therefore MM remains largely incurable.^{4,5} L-PAM resistance is a multifactorial phenomenon attributed to reduced drug accumulation, reduced apoptosis, enhanced DNA repair and enhanced glutathione (GSH)/glutathione-*S*-transferases.^{8–13}

GSH protects MM cells against L-PAM.^{8–10,12} The L-PAM-resistant RPMI-8226/LR-5 cell line demonstrated a twofold increase in GSH and a sevenfold increase in L-PAM IC₅₀ compared with its L-PAM-sensitive counterpart.^{8,10} The increased GSH was attributed to upregulation of the rate-limiting enzyme in GSH synthesis, γ -glutamylcysteine synthetase (γ -GCS).^{10,11} Buthionine sulfoximine (BSO) is a potent inhibitor of γ -GCS.^{12,14–16} BSO enhanced L-PAM activity in the RPMI-8226/LR-5 and RPMI-8226/S MM cell lines,⁸ and in the MOPC-315 murine plasmacytoma.¹⁷ Phase I trials of continuous infusion of BSO induced > 80% depletion of tumor GSH compared with pretreatment levels, but the modest activity of BSO + low-dose L-PAM in adult cancers slowed further clinical development of BSO.^{12,16,18} A high degree of synergistic enhancement of L-PAM cytotoxicity in the presence of BSO was

observed in multidrug-resistant neuroblastoma cell lines, including those that were established at relapse after myeloablative therapy with L-PAM and lines highly resistant to L-PAM due to loss of p53 function, especially at concentrations of L-PAM that were myeloablative.^{19,20} The latter observation led to a recently completed phase I trial of BSO + L-PAM given with stem cell support in the New Approaches to Neuroblastoma Therapy (NANT) consortium that has safely dose-escalated L-PAM given with BSO to myeloablative L-PAM doses, with the stem cell infusions overcoming the expected hematopoietic toxicity (www.NANT.org; www.clinicaltrials.gov, NCT00002730).

Taken together, preclinical and clinical studies in neuroblastoma suggest the potential for BSO to enhance L-PAM activity against diseases that use myeloablative dosing of L-PAM and previous investigations with one murine plasmacytoma,¹⁷ and a human MM cell line,^{8,10} demonstrated enhanced activity of L-PAM by BSO.^{16,21} Therefore, we have undertaken extensive studies to determine the potential for BSO to enhance the anti-myeloma activity of L-PAM at clinically achievable doses using *in vitro* (cell lines and fresh MM explants) and *in vivo* MM xenografts to determine if BSO + L-PAM warrants clinical trials in MM.

MATERIALS AND METHODS

Drugs and chemicals

Powdered L-PAM and BSO (DL buthionine-(*S,R*)-sulfoximine) were purchased from Sigma-Aldrich (St Louis, MO, USA) and clinical grade

¹Cancer Center, School of Medicine, Texas Tech University Health Sciences Center School of Medicine, Lubbock, TX, USA; ²Department of Pharmacology and Neuroscience, Texas Tech University Health Sciences Center School of Medicine, Lubbock, TX, USA; ³Department of Cell Biology and Biochemistry, Texas Tech University Health Sciences Center School of Medicine, Lubbock, TX, USA; ⁴Department of Pediatrics, Texas Tech University Health Sciences Center School of Medicine, Lubbock, TX, USA and ⁵Department of Internal Medicine, Texas Tech University Health Sciences Center School of Medicine, Lubbock, TX, USA. Correspondence: Dr CP Reynolds, Cancer Center, School of Medicine, Texas Tech University Health Sciences Center, 3601 4th Street, Mail Stop 9445, Lubbock, TX 79430, USA.

E-mail: patrick.reynolds@ttuhsc.edu

Received 1 November 2013; revised 8 April 2014; accepted 30 April 2014

BSO (L-buthionine (*S,R*)-sulfoximine (50 mg/ml)) was provided by the National Cancer Institute (Bethesda, MD, USA).²² Interleukin-6, vascular endothelial growth factor, insulin-like growth factor-1 and Annexin V assay kit were from Life Technologies (Carlsbad, CA, USA). F7-26 (mAb) was from Millipore (Billerica, MA, USA).²³ The JC-1 probe, vitamin C, vitamin E, *N*-acetylcysteine (NAC) and sodium thiosulfate (STS) were from Sigma-Aldrich. The anti-CD38 phycoerythrin (PE) and anti-CD138 fluorescein isothiocyanate (FITC) antibodies, and APO-DIRECT kit (terminal deoxynucleotidyl transferase-mediated dUTP nick end labeling (TUNEL)) were purchased from BD Biosciences (San Jose, CA, USA).^{23,24} Caspase-3, caspase-9, poly ADP ribose polymerase and anti-rabbit immunoglobulin G horseradish peroxidase antibodies were from Cell Signaling (Danvers, MA, USA); anti- β -actin was from Santa Cruz Biotechnology (Santa Cruz, CA, USA).

Cell culture

Human MM cell lines MM.1S, RPMI-8226, U266 and NCI-H929 were from ATCC (Manassas, VA, USA) and MOLP-2, KMS-12-PE, OPM-2 and EJM were from DSMZ (Braunschweig, Germany).²⁵ TX-MM-030h (CD38+ and CD138+) was established in our laboratory from a patient with progressive MM after receiving L-PAM-based myeloablative therapy and autologous SCT. EJM and TX-MM-030h were maintained in Iscove's modified Dulbecco's medium, supplemented with 20% fetal bovine serum (FBS) and insulin, selenium, transferrin (BD Biosciences) universal culture supplement (1:1000). MM.1S, RPMI-8226, NCI-H929 and OPM-2 were maintained in RPMI-1640 medium with 10% FBS. U266 was maintained in RPMI-1640 15% FBS, while MOLP-2 and KMS-12-PE were in RPMI-1640 + 20% FBS. All cell lines were grown in antibiotic-free medium and verified to be free of mycoplasma (MycAlert kit, Lonza, Walkersville, MD, USA). Cell line identity was confirmed at the time of experimentation by short tandem repeat genotyping and compared with our database of cell line short tandem repeat profiles (www.TXCCR.org). Cells were cultured and treated in a 37 °C humidified incubator gassed with 5% CO₂ and 90% N₂ so as to achieve bone marrow level hypoxia of 5% O₂ or alternatively room air without N₂ to achieve ~20% O₂.²⁶

Isolation of primary MM cells, bone marrow stromal cell (BMSC) and co-culture

Clinical specimens were obtained with consent via a biobanking protocol approved by the TTUHSC committee for protection of human subjects. Heparinized blood ($n=2$) and bone marrow aspirates ($n=5$) were used to isolate mononuclear cells by Ficoll density gradient centrifugation and cryopreserved using equal volumes of FBS and 15% dimethylsulphoxide dissolved in RPMI-1640 medium.²⁷ The cryopreserved cells were cultured in Iscove's modified Dulbecco's medium supplemented with 20% FBS, insulin, selenium, transferrin, 10 ng/ml of interleukin-6, insulin-like growth factor-1 and vascular endothelial growth factor at 5% O₂ for 1 week before sorting primary MM cells. For sorting, mononuclear cells were reacted with anti-CD38 PE and anti-CD138 FITC antibodies and primary MM cells were isolated using fluorescence-activated cell sorting (BD FACSAria II, San Jose, CA, USA). The percentages of MM cells in mononuclear samples were ~5–60%. Isolated MM cells were cultured in Iscove's modified Dulbecco's medium supplemented with 20% FBS, insulin, selenium, transferrin, 10 μ g/ml of gentamycin, 10 ng/ml of interleukin-6, insulin-like growth factor-1 and vascular endothelial growth factor.²⁸

For preparation of BMSCs, adherent cells were long-term cultured and expanded in Iscove's modified Dulbecco's medium, supplemented with 20% FBS and 10 μ g/ml of gentamycin. BMSC and MM cells co-cultures used ~10⁴ BMSC per well in a 24-well plate overnight before the addition MM cells (10⁵).^{27,28} Once MM cells were attached to the stromal cell layer, BSO was added to the medium. After 24 h of incubation, L-PAM was added. The determination of early apoptosis was done at 24 h by aspirating the MM cells away from the BMSC and using Annexin V assay with flow cytometry and cytotoxicity at 96 h using DIMSCAN assay as previously described.²⁴

DIMSCAN cytotoxicity assay

The cytotoxicity of BSO and L-PAM was determined in a fixed-ratio of concentration (BSO: L-PAM; 8:1) using the DIMSCAN cytotoxicity assay.^{29–31} The drug concentration ranges used were: BSO, 0–400 μ M and L-PAM, 0–50 μ M (clinically achievable levels).^{21,22,32,33} Cells (1–5 \times 10³) or primary MM cells (~10⁴) were seeded, incubated with BSO for 24 h and followed by treatment with L-PAM. After incubating for 96 h with the drugs,

fluorescein diacetate and eosin Y were added to the wells, incubated for 20 min and total fluorescence in each well was measured by DIMSCAN.^{20,24,29}

Determination of total GSH (GSH + GSSG) using high-performance liquid chromatography

Intracellular GSH and GSSG levels were measured using a published method.³⁴ A derivatization procedure was used using phthalaldehyde. The separation of derivitized GSH was achieved using a mobile phase consisting ammonium formate buffer (0.1 M pH 6.0)—methanol 100% (60:40 v/v) at the flow rate of with 0.5 ml/min using the C18 column (Agilent Zorbax Eclipse, Santa Clara, CA, USA; 150 \times 4.6 mm, 3.5 μ m). The eluted derivatives of GSH were detected at an excitation wavelength of 340 nm and an emission wavelength of 420 nm. The calibration curve was linear over the range 0.156–20 μ g/ml with the correlation coefficient >0.995.

Determination of single-strand DNA (ssDNA) breaks, mitochondrial membrane depolarization, caspase cleavage and DNA fragmentation

Cells were seeded, pretreated with BSO (400 μ M) for 24 h followed by treatment with L-PAM (30 μ M). Determination of ssDNA breaks,²³ mitochondrial membrane depolarization,²⁴ caspase cleavage²⁴ and apoptotic DNA fragmentation²³ was carried out as previously described.^{23,24}

In vivo activity testing against human MM xenografts

Studies were carried out in the TTUHSC Laboratory Animal Resources Center under protocols approved by the Institutional Animal Care and Use Committee. Six- to eight-week-old female NCI *beige-nude-xid* (Bethesda, MD, USA) mice were subcutaneously inoculated between shoulder blades with 25–30 \times 10⁶ MM cells using matrigel (BD Biosciences). When tumors achieved a size of \geq 100 mm³, mice were randomized into four groups. BSO (50 mg/ml) was diluted in sterile 0.9% w/v saline. Powdered L-PAM was dissolved in 0.1 N HCl ethanol and diluted in saline immediately before injection. Controls received vehicle only, BSO-only group received 125 mg/kg twice daily on days 1, 2 and 3 via intraperitoneal injection, L-PAM-only group received 10 mg/kg dose on days 2 and 3 given intravenously into the lateral tail vein, and the L-PAM + BSO group received both drugs as per above. Tumor volume was measured twice weekly using the formula $\frac{1}{2}$ length \times breadth \times height.^{35,36} Mice were weighed twice weekly to assess toxicity and killed when tumors reached 1500 mm³ or they experienced any severe morbidity (that is, body weight <17 g).

Determination of responses and event definitions for MM subcutaneous xenograft model

Responses were assessed as previously described.³⁷ Complete response (CR) was defined as disappearance of a measurable tumor mass (<50 mm³) for at least one time point; a CR was considered as a maintained (maintained CR (MCR)), if maintained (<50 mm³) for 100 days. Partial response was defined as tumor volume regression \geq 50% from initial volume for at least one time point during therapy but with a measurable tumor mass. Mouse event-free survival (EFS) was calculated as the number of days from treatment initiation until the tumor volume reached 1500 mm³, death from any cause or morbidity that required killing. An EFS T/C was calculated as the ratio of median time to event of the treatment group to the median time to event of the controls. High activity was: (a) EFS T/C ratio >2, (b) a significant difference ($P<0.05$) was observed in the EFS distribution between treatment and control groups and (c) a net reduction in tumor volume in treated vs controls at the end of treatment was observed. Agents meeting the first two criteria but not having a net reduction in the median tumor volume for treated animals at the end of study were considered as moderately active. An EFS T/C <2 was regarded as low activity. Relative tumor volume (RTV) was calculated when all or a majority of mice in control and treatment group had a measurable tumor (days 8–9). The tumor volume T/C value was the mean RTV for the treatment group to that of mean RTV for control group. Agents producing T/C of <45% were regarded as highly active, 45–60% were considered to have moderate activity and >60% were considered to have low activity.

RESULTS

BSO synergistically enhanced L-PAM-induced cytotoxicity in nine MM cell lines, in presence of BMSC and MM cytokines, and in seven primary MM cells

We determined the cytotoxicity of clinically achievable levels of BSO (0–400 μM) and L-PAM (0–50 μM) in nine human MM cell lines using the DIMSCAN cytotoxicity assay (Figure 1a). L-PAM as a

single agent was highly active against MM.1S, KMS-12-PE, MOLP-2 and NCI-H929, inducing ≥ 2 logs of cell kills at the maximum dose (50 μM). In the remaining five cell lines, L-PAM showed modest activity and induced ≤ 2 logs of cell kill. BSO alone had minimal to no activity in six cell lines and had modest activity in the OPM-2, KMS-12-PE and MM.1S lines. The combination of BSO + L-PAM achieved synergistic cytotoxicity (combination index number (CIN)

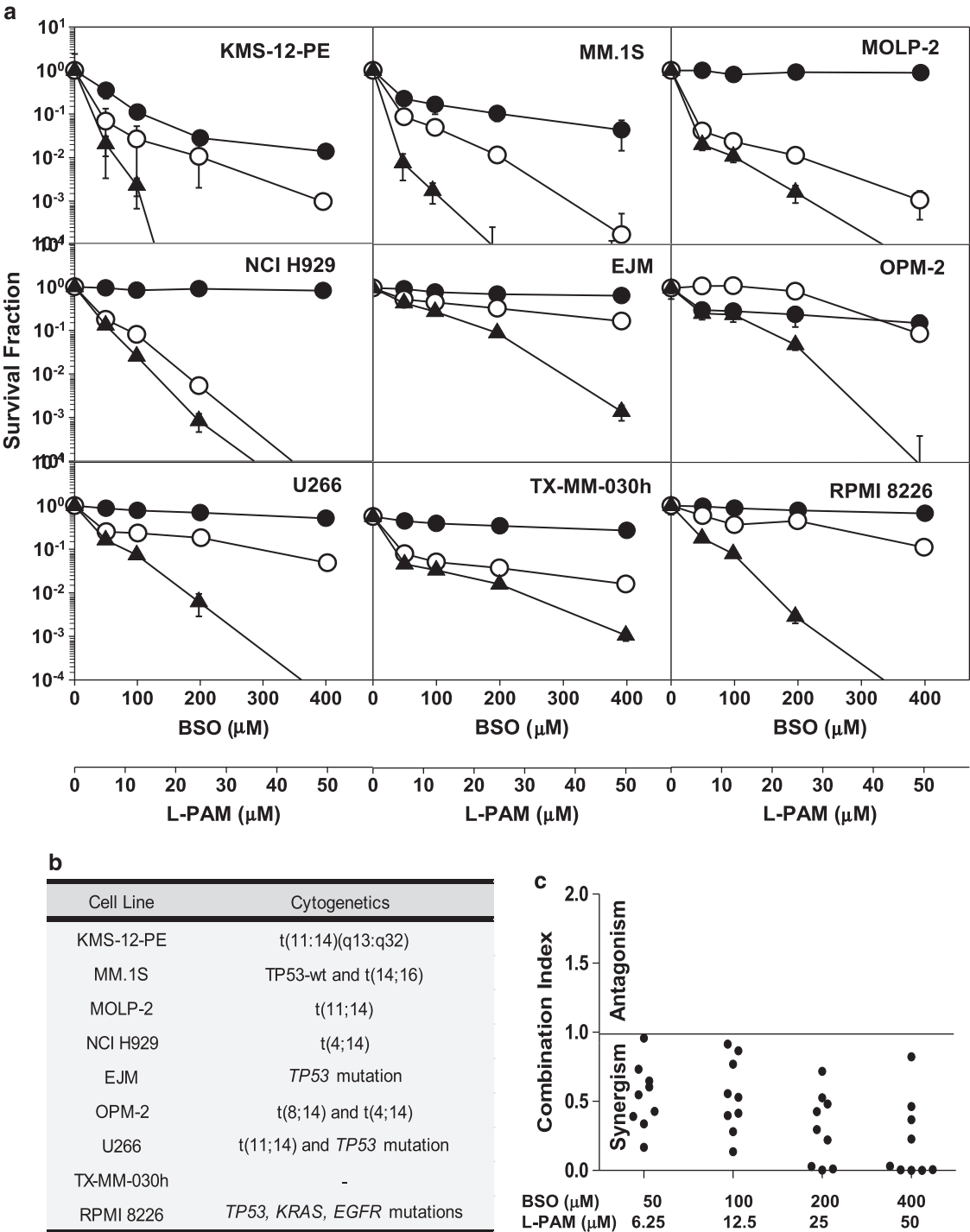


Figure 1. Representative dose response curves of BSO (black circles), L-PAM (white circles) and BSO + L-PAM (black triangles) in nine MM cell lines. **(a)** Drug concentrations were 0–400 μM for BSO and 0–50 μM for L-PAM (Fixed ratio, BSO: L-PAM: 8:1). Cultures were treated with BSO for 24 h, at which time L-PAM was added, followed by 96 h of incubation before DIMSCAN cytotoxicity analysis. Cell lines were cultured in bone marrow level hypoxia (5% O₂). The survival fraction was determined by mean fluorescence of the treated cells/mean fluorescence of control cells. Error bars represent s.d. ($n \geq 3$). **(b)** Summary of cytogenetic abnormality of MM cell lines **(c)** CINs were calculated for fixed ratio of BSO and L-PAM (8:1) using CalcySyn software (Biosoft, Cambridge, UK). The CIN values < 1 indicate synergism and > 1 indicate antagonism effect.

≤ 0.7) and induced 2–4 logs of cell kill in all nine MM cell lines including the eight lines established at progressive disease (PD) after therapy (U266, OPM-2, NCI H929, KMS-12-PE, EJM, TX-MM-030h, MM.1S and MOLP-2),²⁵ which include lines with cytogenetic profiles associated with a poor prognosis (Figure 1b).^{25,38,39} The combination of BSO (200 μM) and L-PAM (25 μM) achieved very strong synergism (CIN ≤ 0.1) in RPMI-8226 (*TP53*, *KRAS* and *EGFR* mutations) and U266 (*TP53*-mutation) cell lines,^{38,40} and strong synergism (CIN 0.1–0.3) was seen in MM.1S (*TP53*-wt and t(14;16)), KMS-12-PE (t(11;14) (q13;q32)) and EJM (*TP53*-mutation).^{25,38,40} BSO + L-PAM was synergistic (CIN 0.3–0.7) in OPM-2 (t(4;14)(p16;q32)), NCI-H929 (t(4;14)) TX-MM-030h (post-BMT) and MOLP-2 (t(11;14)(q13;q32))³⁹ cell lines (Figures 1a–c).^{25,38} Identical results were also obtained for all

cell lines tested with BSO + L-PAM when cultured in 'standard' culture conditions (room air + 5% CO_2 ; Supplementary Figure 1).

We assessed whether the activity of BSO + L-PAM is attenuated by co-culture with MM cytokines (interleukin-6, insulin-like growth factor-1 and vascular endothelial growth factor) and BMSCs. In all four cell lines tested, BSO + L-PAM significantly ($P < 0.05$) enhanced % apoptotic cells (Annexin V+ and PI+/–) as compared with L-PAM (Figure 2a). Similar to the observation in MM cell lines, the combination treatment induced multi-logs of synergistic cell kill (CIN < 1.0) (Figures 2b and c). Next, we determined the efficacy of BSO + L-PAM in freshly isolated primary MM cells from clinical specimens. Consistent with the effects in MM cell lines, pretreatment with BSO synergistically (CIN < 1.0) enhanced L-PAM-induced cytotoxicity in all primary

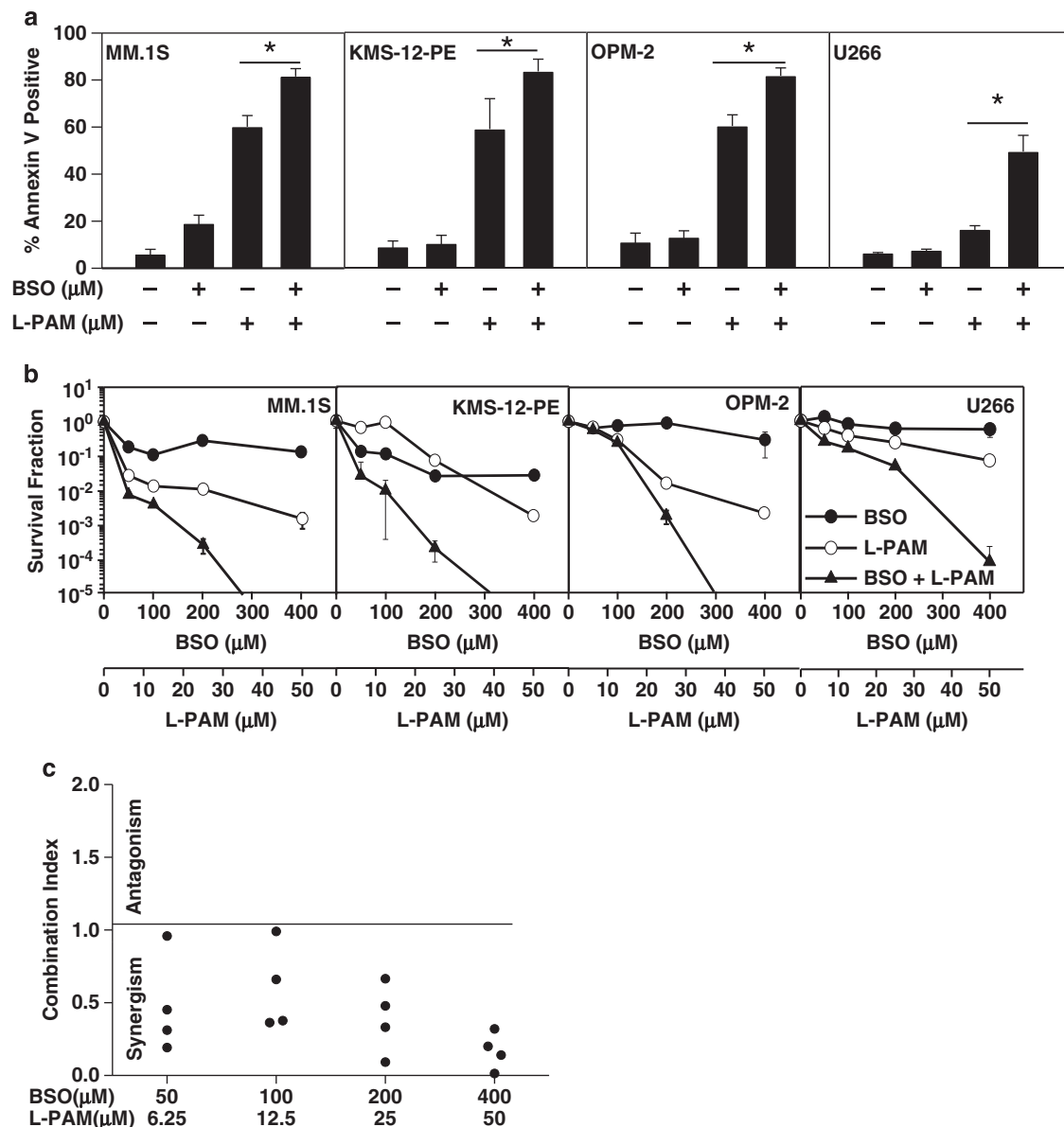


Figure 2. Four MM cell lines were cultured in presence of BMSCs and MM cytokines (interleukin-6 (IL-6), vascular endothelial growth factor (VEGF) and insulin-like growth factor-1 (IGF-1)) at the concentrations of 10 ng/ml. **(a)** The percentage of apoptosis in MM cells (aspirated away from the BMSC) was determined using Annexin V assay and flow cytometry at 24 h after the treatment with BSO (400 μM) and L-PAM (30 μM). Bars represent percentage of cell undergoing apoptosis (Annexin V+ and PI+/–). Error bars represent s.d. ($n \geq 3$) and asterisk represent statistical difference in means ($P < 0.05$). **(b)** Cells were treated with BSO (0–400 μM), L-PAM (0–50 μM) and BSO + L-PAM. At the end of 96 h, MM cells were carefully aspirated off of the BMSC, plated in 96-well plates, and assayed for cytotoxicity using DIMSCAN. Error bars represent s.d. ($n \geq 3$). **(c)** The CINs were determined using for the fixed ratio of BSO and L-PAM (8:1).

MM cells, including in samples obtained from patients who had significant prior exposure to chemotherapy and had SCT (Figures 3a–c).

BSO enhanced L-PAM-induced ssDNA breaks and mitochondrial depolarization

To understand the mechanism of enhanced cytotoxicity of L-PAM in the presence of BSO, we determined ssDNA breaks induced by L-PAM ± BSO.²³ In all four cell lines tested, BSO significantly increased ($P < 0.05$) L-PAM-induced ssDNA breaks compared with L-PAM only (Figures 4a and b). For instance, in the MM.1S cell line, the cells with ssDNA breaks (Figure 4a, quadrant 4; FITC +/PI –) showed $5.2 \pm 0.2\%$ in controls, $8.6 \pm 0.4\%$ with $400 \mu\text{M}$ of BSO treatment, $50.19 \pm 1.3\%$ in presence of $30 \mu\text{M}$ of L-PAM and

$64.6 \pm 2.2\%$ with BSO + L-PAM ($P < 0.05$). Similarly, in OPM-2, KMS-12-PE and U266 cell lines, BSO + L-PAM significantly increased ($P < 0.05$) ssDNA breaks relative to single agents and controls.

As apoptosis has been reported as a primary mechanism of action for BSO and L-PAM,^{13,19} we determined if enhanced cytotoxicity from the combination was due to increased apoptosis by assessing loss of mitochondrial membrane potential.^{24,41,42} In all four cell lines tested, we observed a significant loss ($P < 0.05$) in mitochondrial membrane potential because of BSO + L-PAM treatment as compared with single agents or controls (Figures 4c and d). For example, in the MM.1S cell line, the percentage of cells with depolarized mitochondria were $10.9 \pm 9.5\%$ in controls, $10.2 \pm 8.1\%$ with BSO alone, $45.2 \pm 5.3\%$ with L-PAM alone and $63.7 \pm 5.7\%$ with BSO + L-PAM, ($P < 0.05$ for BSO + L-PAM relative to single agents and controls).

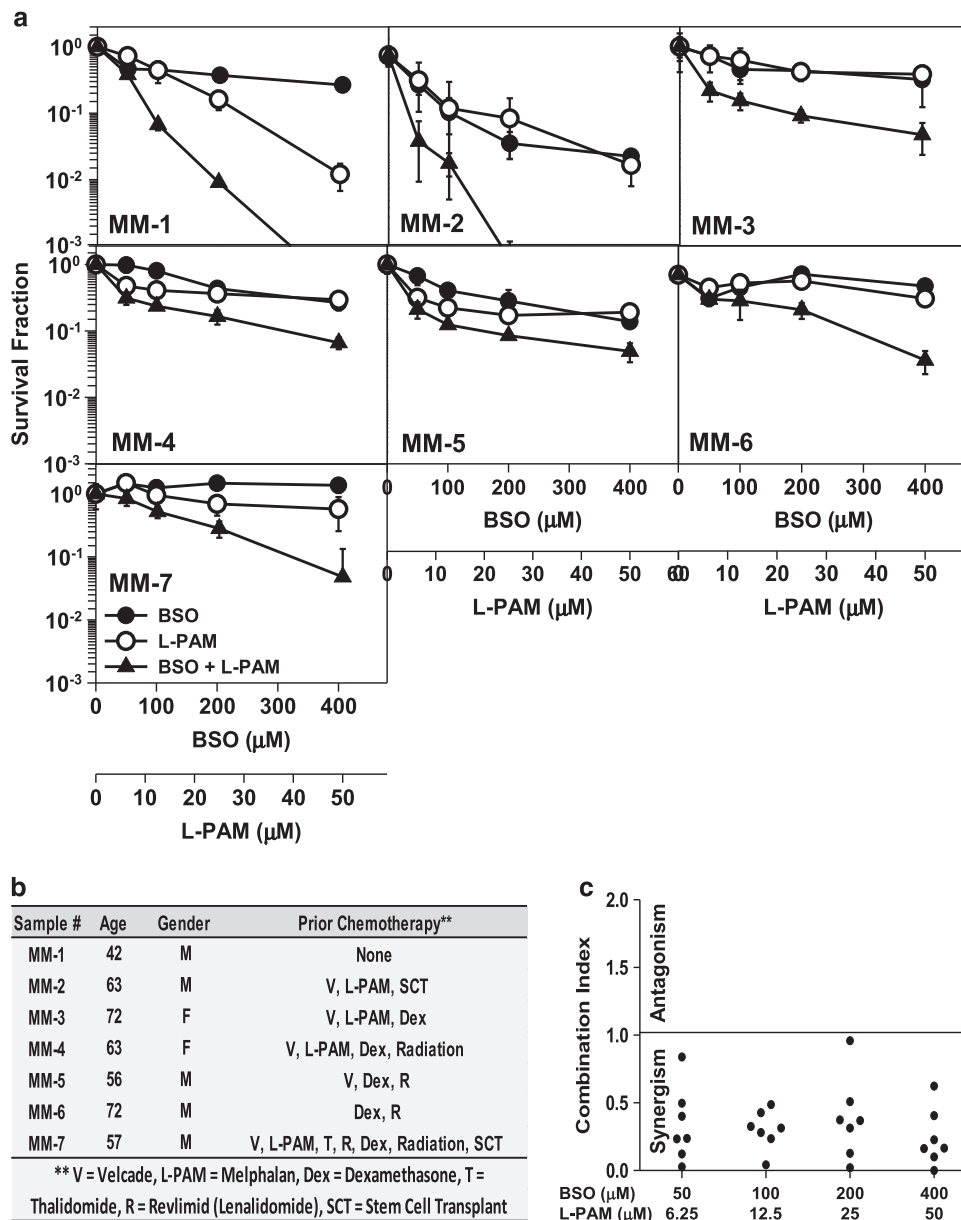


Figure 3. Anti-myeloma activity of BSO and L-PAM as a single agent and combination in primary MM cells when cultured with MM cytokines at bone marrow level hypoxia. **(a)** Dose-response curves of BSO (black circles), L-PAM (white circles) and combination (black triangles). Primary MM cells were seeded ($\sim 10\,000$), treated with BSO (0 – $400 \mu\text{M}$) for 24 h followed by the treatment with L-PAM (0 – $50 \mu\text{M}$). The cytotoxicity was determined using DIMSCAN assay at 96 h of incubation with the drugs. Error bars represent s.d. ($n \geq 3$). **(b)** List of relevant clinical information of MM samples. Each sample was collected from different patients. Except for MM-1 all samples were collected from patient who had significant exposure to chemotherapy. **(c)** The CIN numbers were calculated as described in Figures 1 and 2.

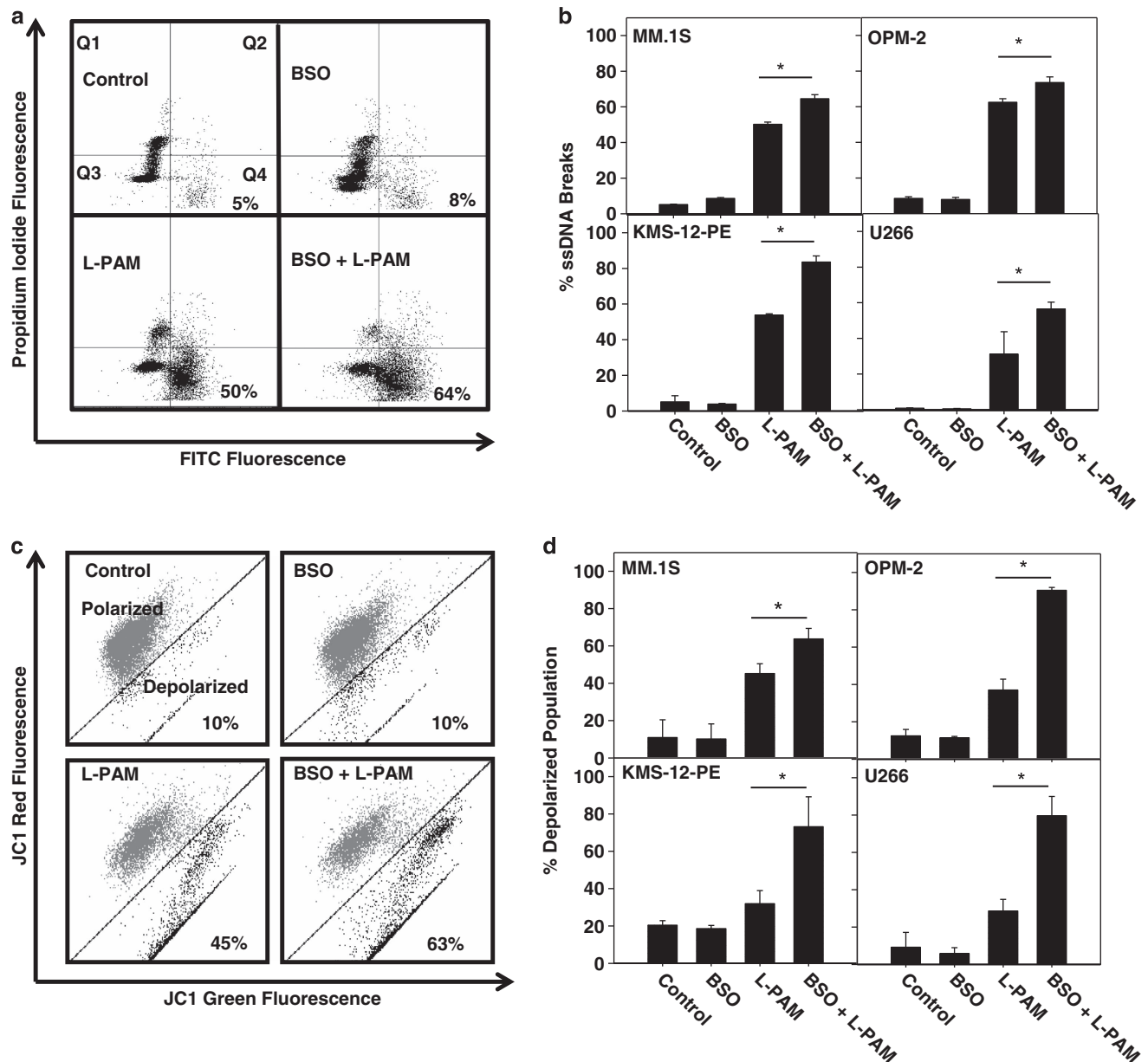


Figure 4. Measurement of ssDNA breaks (F7-26 mAb) and mitochondrial depolarization (JC 1) by flow cytometry in four MM cell lines. **(a)** MM.1S cells were pretreated with BSO (400 μ M) followed by L-PAM (30 μ M) for 24 h, collected, fixed, incubated with 2 μ g of F7-26 mAb, followed by incubation with 1 μ g of FITC-conjugated goat anti-mouse IgM antibody, and counterstained with propidium iodide (PI). Data were acquired using a BD LSRII flow cytometer and FACS Diva software (San Jose, CA, USA). Doublet discrimination were used using two parameter cytograms with PI = DNA content area measurement vs PI width measurement. Spectral overlap was determined between FITC and PI and all experiments were performed using compensation. High-FITC fluorescence (quadrants 3 + 4) was an indicator of cells with significant ssDNA breaks. **(b)** In all four cell lines, BSO + L-PAM significantly enhanced ($P < 0.05$) ssDNA breaks as compared with single agents and controls. The bars represent mean % ssDNA breaks (\pm s.d.) and asterisk represents statistical difference in mean ($P < 0.05$; $n = 3$). **(c)** MM.1S cells were treated, stained with 2 μ M of JC1 for 30 min at 37 $^{\circ}$ C and analyzed using flow cytometry. The depolarization is indicated by the transition from red (shown in gray) to green (shown in black) fluorescence. **(d)** In all four cell lines tested, BSO + L-PAM significantly enhanced ($P < 0.05$) mitochondrial depolarization as compared with single-agent treatment and control.

BSO increased L-PAM-induced cleavage of caspase-9, caspase-3, poly ADP ribose polymerase and apoptosis

Mitochondrial membrane depolarization is accompanied by the discharge of cytochrome-c, formation of apoptosomes and cleavage of procaspase-9 to caspase-9.^{41,42} Activation of caspase-9 initiates the cascade of caspases and cleavage of critical intracellular proteins.⁴¹ In the MM.1S, RPMI-8226 and U266 cell lines, L-PAM \pm BSO enhanced cleavage of caspase-9, caspase-3

and PARP relative to control and single agents (Figure 5a and Supplementary Figure 3). We also examined internucleosomal DNA fragmentation induced by BSO + L-PAM using the TUNEL assay.^{41,42} Consistent with our data for caspase activation, BSO significantly increased apoptosis induced by L-PAM in all cell lines tested ($P < 0.05$; Figures 5b and c), although the enhanced apoptosis in the MM.1S and KMS-12-PE lines was modest in comparison with the synergistic cytotoxicity (Figure 1) suggesting

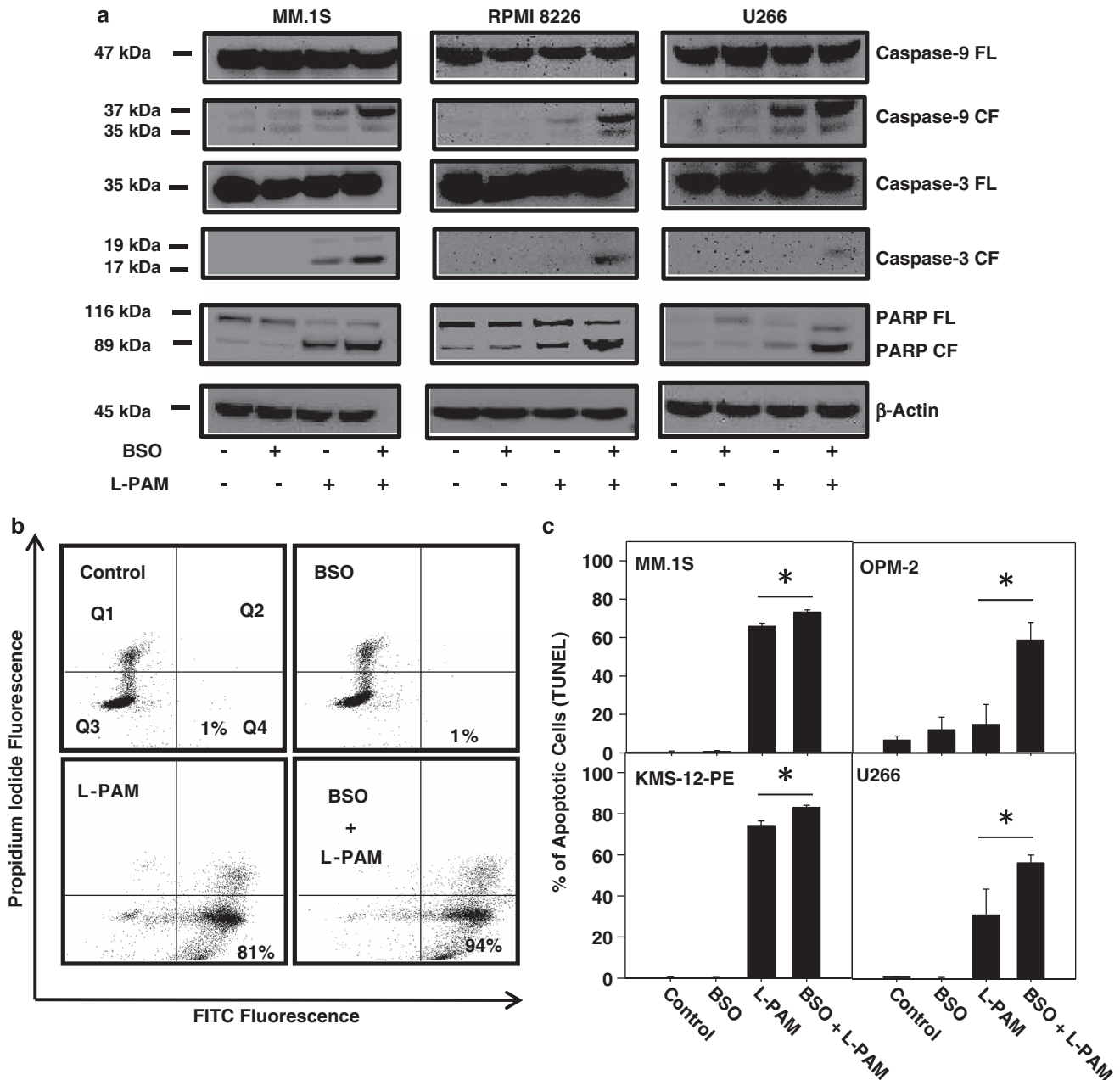


Figure 5. BSO + L-PAM treatment induced a significant increase in cleavage of caspase-9, caspase-3, poly ADP ribose polymerase (PARP), and apoptosis (TUNEL). (a) The MM.1S, RPMI-8226 and U266 cell lines were treated with BSO for 24 h, followed by L-PAM treatment for 24 h. Cells were lysed, sonicated and centrifuged at 13 000 *g* for 30 min and 50 μ g of protein (supernatant) in each sample was resolved by electrophoresis using 4–12% bis-tris gels, transferred to polyvinylidene difluoride membrane, incubated with antibodies and visualized by enhanced chemiluminescent substrate. β -Actin served as a loading control. Full-length caspase-9 is 47 kDa protein that is cleaved into 37 and 35 kDa fragment due to L-PAM \pm BSO treatment. Similarly, caspase-3 (35 kDa) gets cleaved into a small fragment (17/19 kDa), whereas PARP, a 116 kDa protein, forms a large fragment (89 kDa) upon cleavage by caspase-3. (b) MM.1S cells were treated with vehicle, BSO (400 μ M), L-PAM (30 μ M) and BSO + L-PAM, collected 48 h after stimulation, fixed, incubated with TdT enzyme and FITC-dUTP for 2 h, counterstained with propidium iodide and analyzed with flow cytometry as described in Figure 4a. Cells in quadrant-4 (Q4, FITC + /PI –) were considered to be apoptotic. (c) BSO + L-PAM treatment significantly enhanced ($P < 0.05$) percentage of apoptotic cells as compared with single-agent treatment in MM.1S, KMS-12-PE, OPM-2 and U266 cell lines. Apoptosis data are from flow cytometry analysis as depicted in Figure 5b. The bars represent mean % apoptosis (\pm s.d.) and asterisk represents statistical difference in mean ($P < 0.05$).

non-apoptotic mechanisms may account for much of the BSO enhancement in these lines. Apoptosis as a mechanism of synergistic cytotoxicity was confirmed by demonstrating that inhibition of caspase cleavage by pan-caspase inhibitor QVD-OPH significantly reversed the cytotoxicity and apoptosis induced by BSO + L-PAM (Supplementary Figures 4 and 5).

BSO significantly depleted GSH *in vitro* and *in vivo* and L-PAM treatment induced GSH extrusion

BSO significantly ($P < 0.05$) depleted GSH in all nine cell lines (Figure 6a). The mean GSH in controls was 51.4 ± 33.4 ng/mg, which decreased to 10.4 ± 5.6 ng/mg. *In vivo*, BSO significantly depleted GSH in xenografted MM cells (control = 10.2 ± 1.4 ng/mg

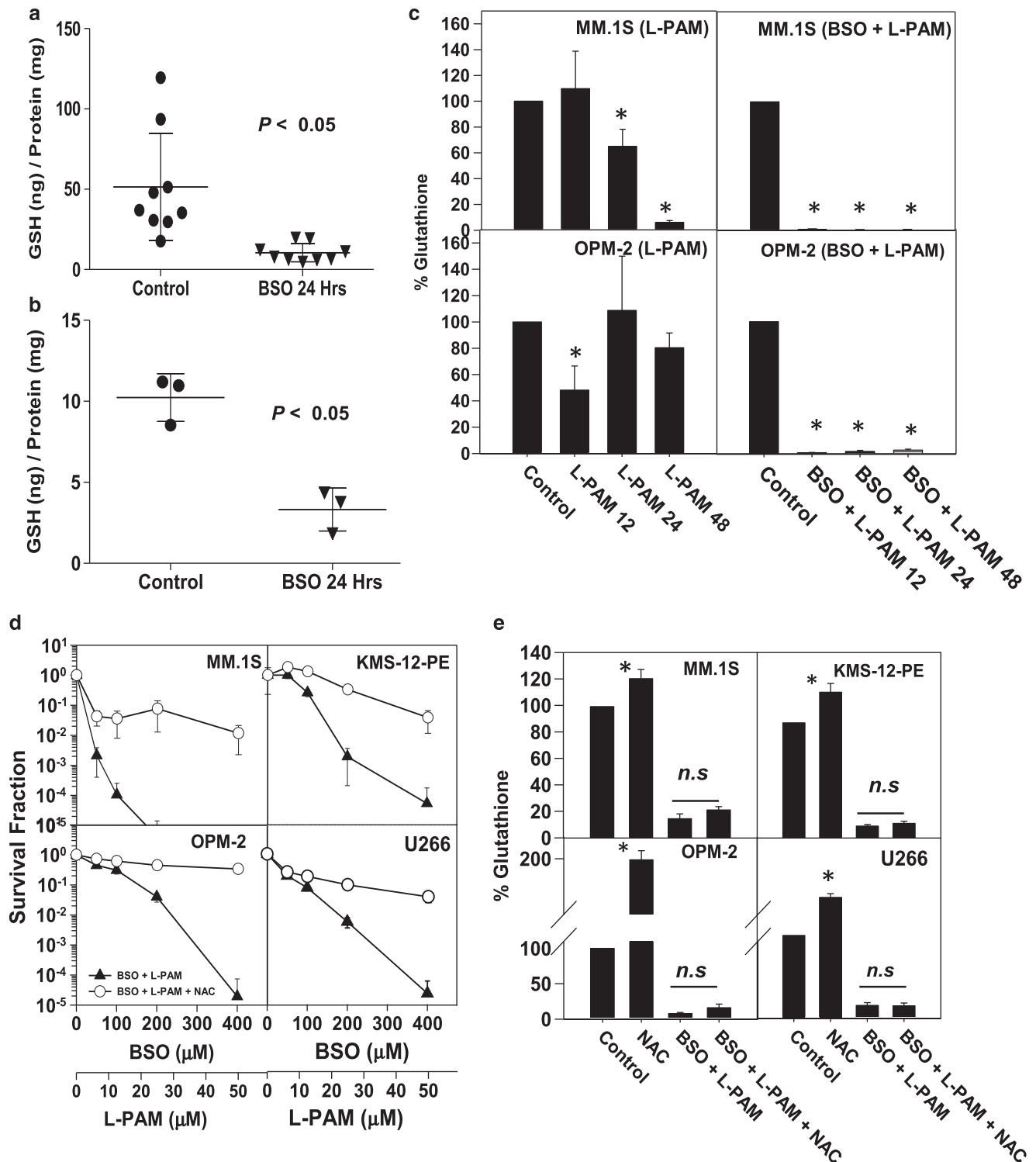


Figure 6. Effect of BSO and L-PAM treatment on total GSH (GSH + GSSG). **(a)** The bars represent the mean GSH (GSH + GSSG) in individual cell lines \pm BSO (400 μM) treatment for 24 h. The error bars represent s.d. **(b)** In a separate experiment, NCI-BNX mice were inoculated with MM.1S cell line. When progressively growing tumors were $\geq 100 \text{ mm}^3$, mice were treated with 125 mg/kg b.i.d of BSO (total dose 250 mg/kg). At 12 h after the last dose, mice were killed, tumors from controls ($n = 3$) and BSO-treated mice ($n = 3$) were harvested, minced and total GSH was determined as described in methods. Consistent with the *in vitro* data, BSO significantly depleted GSH in MM cells *in vivo*. **(c)** MM.1S (L-PAM sensitive, $\text{IC}_{90} = 12.5 \mu\text{M}$) and OPM-2 (L-PAM-resistant $\text{IC}_{90} = 52 \mu\text{M}$) were treated with L-PAM alone (10 μM) or BSO + L-PAM (400 μM + 10 μM) and total GSH levels were determined using high-performance liquid chromatography (HPLC). The total GSH levels were normalized using total protein content. Bars represent % of GSH compared with control and error bars represent s.d. ($n = 3$). Asterisk represents statistical difference in the means ($P < 0.05$). **(d)** Cells were seeded, treated with BSO for 24 h, NAC (750 or 1000 μM) was added 3 h before the treatment with L-PAM (0–50 μM) and cells were incubated with drugs for 96 h and the survival fraction was determined using DIMSCAN assay. **(e)** Cells were seeded, treated with NAC alone (750 or 1000 μM), or BSO + L-PAM (400 μM + 10 μM) or NAC + BSO + L-PAM. The total GSH was determined as described in Materials and Methods section. Bars represent % GSH compared with control and error bars represent s.d. ($n = 3$) (NS, not significant).

vs treated 3.3 ± 1.3 ng/mg, $P < 0.05$) (Figure 6b). We also investigated the effect of L-PAM on intracellular GSH in MM.1S (L-PAM-sensitive, IC_{50} : $12.5 \mu\text{M}$) and OPM-2 (L-PAM-resistant, IC_{50} : $52.5 \mu\text{M}$) cell lines. L-PAM treatment significantly ($P < 0.05$) depleted GSH in the MM.1S cell line at 24 and 48 h (Figure 6c). In OPM-2, GSH was significantly depleted at 12 h, recovered by 24 h and maintained at 48 h. However, BSO treatment abolished ability of OPM-2 to recover GSH that was depleted by L-PAM (Figure 6c).

Treatment with NAC antagonized the synergistic cytotoxicity of BSO + L-PAM

To determine if the action of BSO in enhancing L-PAM cytotoxicity was due to the decreased GSH removing a key intracellular absorbent of L-PAM, we assessed the cytotoxicity of BSO + L-PAM in the presence of the thiol NAC. As shown in Figure 6d, pretreatment with NAC substantially reversed the cytotoxicity induced by BSO + L-PAM in all four cell lines. Highest reversal was seen in L-PAM-resistant OPM-2 and U266 cell lines. To understand this observation, we analyzed the GSH levels with NAC \pm BSO + L-PAM treatment. NAC treatment enhanced ($P < 0.05$) the basal GSH levels by $\geq 25\%$. However, in the presence of BSO, NAC failed to enhance GSH levels because of the potent inhibition of the γ -GCS by BSO. This observation suggests that protective effect of NAC is likely to be mediated by GSH-independent mechanisms.⁴³ We also observed that treatment with STS substantially reversed the effect of BSO + L-PAM, but for most MM lines non-thiol antioxidants (vitamins C and E) did not alter the cytotoxic synergy of BSO + L-PAM (Supplementary Figure 6). These latter data indicate that the antagonism of BSO + L-PAM by NAC and STS is not due to their antioxidant properties or a restoration of GSH, but likely the thiols (like GSH) bind to and de-toxify L-PAM.

In MM xenografts, BSO + L-PAM increased apoptosis, induced CRs and doubled median EFS relative to L-PAM alone

To determine the activity of BSO + L-PAM *in vivo*, we established subcutaneous xenografts in immunocompromised mice from the MM.1S, OPM-2 and KMS-12-PE cell lines. For all three MM xenograft models, BSO alone had very low or no activity (RTV $> 60\%$ and EFS T/C < 2) and failed to induce any objective responses (Figures 7a and b and Table 1). All mice in control and BSO-treated groups showed PD. In the MM.1S xenograft model, L-PAM as a single agent was highly active (RTV = 11.2% and EFS T/C = 2.5), inducing partial responses in 8/10 and PD in 2/10 mice. In the OPM-2 xenografts, L-PAM had low activity (RTV = 63.9% and EFS T/C = 1.8), with PD observed in 3/5 mice, partial response in 1/5 and CR in 1/5 mice. In the KMS-12-PE xenografts, L-PAM alone was moderately active (RTV = 45.3% and EFS T/C = 1.7) and induced a CR in one mouse (1/6), while the other five mice had PD. In contrast to controls and mice treated with single agents, BSO + L-PAM had potent activity in all three MM xenograft models (RTV $< 45\%$ and EFS T/C > 2). In MM.1S xenografts, BSO + L-PAM induced CRs in all 10 mice and 1 mouse had a maintained CR (MCR) (CR ≥ 100 days). In two of the OPM-2 xenografts, BSO + L-PAM reduced tumor volumes of 1330 mm^3 and 972 mm^3 to $< 50 \text{ mm}^3$ within 33 and 19 days, respectively, and induced CRs in 7/7 mice, of which 5/7 were MCRs. In KMS-12-PE xenografts, 4/8 mice had CRs, 2/8 had partial responses and 2/8 had PD (Figure 7a and Table 1). BSO + L-PAM treated mice lost $\sim 23\%$ of initial body weight but regained weight during the third week (Supplementary Figure 2).

The median EFS of control groups were 9, 10 and 10 days in MM.1S, OPM-2 and KMS-12-PE, respectively (Table 1). BSO alone did not induce any objective responses and the median EFS was not significantly different than controls (MM.1S, OPM-2 and KMS-12-PE, median EFS = 11, 13 and 10 days, respectively). In MM.1S xenografts, L-PAM alone increased the median EFS by 2.5-fold and 2.0-fold relative to controls and BSO, respectively. In the OPM-2

xenografts, L-PAM alone induced a 1.8-fold increase (18.0 days) in the median EFS relative to controls (10 days) and 1.3-fold relative to BSO alone (13 days). In KMS-12-PE, the median EFS after L-PAM single-agent treatment were increased by 1.7-fold (17.5 days) as compared with controls (10 days) and BSO (10 days).

In MM.1S xenografts, BSO + L-PAM treatment increased the median EFS by 5.8-fold over controls, 4.8-fold compared with BSO and 2.3-fold relative to L-PAM alone ($P < 0.001$; Figure 7b and Table 1). For OPM-2 xenografts, BSO + L-PAM enhanced median-EFS to 100 days, a 10-fold increase compared with the control group, 7.6-fold over BSO alone and 5.5-fold compared with L-PAM alone ($P < 0.001$). In KMS-12-PE xenografts, the median EFS for BSO + L-PAM was increased by 4.4-fold over controls and BSO alone and 2.5-fold compared with L-PAM alone ($P < 0.001$). For all three xenograft models, log-rank analysis showed that BSO + L-PAM treatment significantly enhanced ($P < 0.001$) the median EFS as compared with either single agent or the controls. Combining survival analysis data from all models demonstrated that BSO + L-PAM treatment had a very high activity (RTV $< 45\%$ and EFS T/C > 2), inducing CRs in majority of the mice treated (21/25), achieving MCRs in 6/25 mice, and doubling the median EFS relative to L-PAM alone ($P < 0.001$; Figure 7b and Table 1). We analyzed tumor sections from MM xenografts using TUNEL immunohistochemistry and found that BSO + L-PAM treatment significantly enhanced ($P < 0.05$) the fraction of apoptotic nuclei ($82 \pm 21.7\%$) as compared with controls ($2.1 \pm 2.4\%$), BSO alone ($3.6 \pm 3.5\%$) and L-PAM alone ($13.1 \pm 11.1\%$) (Figures 7c and d).

DISCUSSION

Survival of MM patients has improved significantly since the introduction of proteasome inhibitors and immunomodulatory drugs.^{2,44} However, nearly all treated patients either suffer a relapse or develop refractory disease.^{1,4-7,44-47} The outcome of treatment in patients relapsed from bortezomib and thalidomide or lenalidomide remains poor with a median overall survival of 9 months and EFS of 5 months.^{7,47} Furthermore, only 44% of patients achieved a minimal or better response to post-relapse treatment, while others either have stable disease, progression or no response.⁷ Thus, MM remains a largely incurable disease and therefore there is a need to develop new strategies for treating MM.⁴⁻⁷

Alkylating agents are common drugs in MM therapy either as part of induction regimen (cyclophosphamide) or for myeloablative therapy (L-PAM) before SCT.^{2,33,44} The frequent relapses with progressive declines in response rates and duration of response to salvage therapy^{1,2,5-7,45,46} indicate the development of drug resistance,^{1,5,45} suggesting that exploration of novel drug combinations with ability to overcome resistance to conventional drugs is one promising approach with the potential to improve the outcome of existing treatment.^{8,12,20} Of several known mechanisms of resistance,^{8,9,13} increased intracellular GSH has been shown to be associated with L-PAM resistance in MM,^{8,10} and is mainly attributed to upregulation of the γ -GCS enzyme.¹⁰ BSO is a potent and specific inhibitor of γ -GCS, originally synthesized by Griffith *et al.*^{14,15} which has been shown to enhance the anti-myeloma activity of L-PAM in sensitive (8226/S) and resistant (8226/LR5) MM cell lines.⁸ Although this later study demonstrates chemosensitization to L-PAM by BSO in MM, it was limited to one cell line from one patient, testing took place in non-physiological hyperoxic room air conditions,^{8,26} and BSO + L-PAM activity was not assessed *in vivo*. Furthermore, the dose of BSO used was $\sim 1/5$ th (100 μM) of the clinically achievable levels, as clinical studies in adults have demonstrated that continuous infusion of BSO safely achieved $\sim 500 \mu\text{M}$ levels when given with L-PAM.^{12,16,21} Dorr *et al.*¹⁷ demonstrated that pretreatment with BSO enhanced the activity of L-PAM in a murine plasmacytoma model, but the activity in human MM xenografts has not been previously explored.

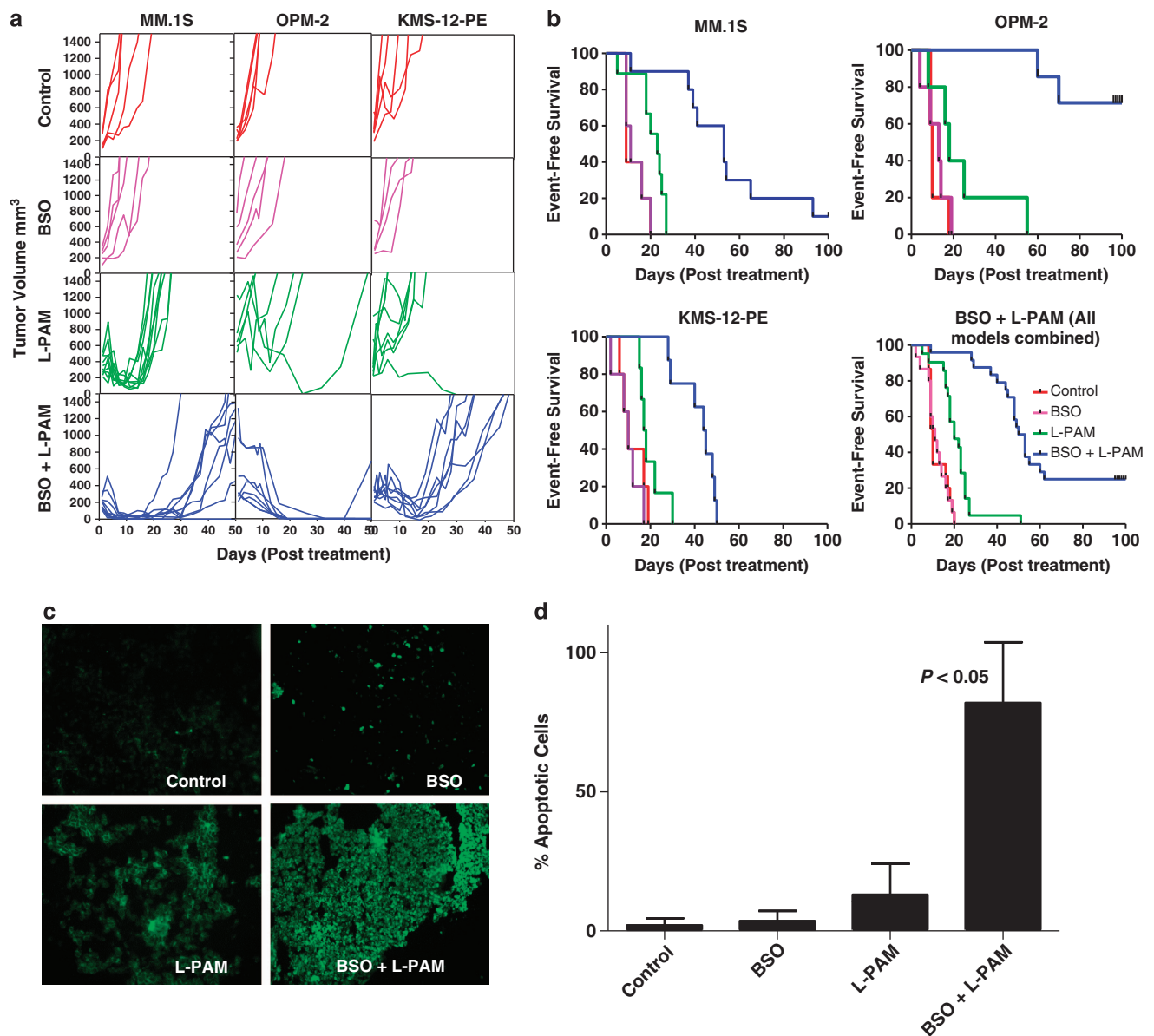


Figure 7. BSO + L-PAM treatment induced CRs, and increased the median-EFS relative to L-PAM or BSO alone in MM xenografts. **(a)** *In vivo* activity of L-PAM in combination with BSO against three human MM lines as murine xenografts. NCI BXH mice carrying, MM.1S, OPM-2 and KMS-12-PE subcutaneous xenografts were treated with BSO (125 mg/kg b.i.d for days 1, 2 and 3) and L-PAM (10 mg/kg/day for days 2 and 3) as single agents or in combination. Tumor volumes were measured twice weekly. Individual lines represent tumor volume in a mouse after initiation of treatment (day 1). Mice were killed when reaching the defined end point (tumor volume $\geq 1500 \text{ mm}^3$). A CR was defined as tumor volume $\leq 50 \text{ mm}^3$ and a MCR was defined as a CR that persisted for 100 days. Each group had at least five mice. The study was terminated after 100 days of initiating treatment and all surviving mice were humanely killed by cervical dislocation. **(b)** The mouse EFS was calculated as time from initiating treatment until the end point (tumor volume $\geq 1500 \text{ mm}^3$ or severe morbidity). The survival distribution for each cohort was compared using the log-rank test using GraphPad Prism software (La Jolla, CA, USA). BSO + L-PAM induced >4 -fold increase ($P < 0.001$) in median-EFS as compared with controls and >2 -fold increase ($P < 0.001$) as compared with L-PAM in MM.1S xenograft, in OPM-2, in KMS-12-PE and for all models combined. **(c)** Analysis of apoptosis (TUNEL staining) in xenograft MM tumors after BSO + L-PAM treatment. MM.1S xenograft mice were treated as described in Materials and Methods section. Tumors were harvested 4–5 days after last treatment, fixed in formalin, embedded in OCT compound (Tissue Tek, Torrance, CA, USA) and sectioned using a cryostat. The *In Situ* Cell Death Detection Kit (Roche Applied Sciences, Indianapolis, IN, USA) was used for TUNEL staining. Images were obtained using a fluorescent microscope (Olympus, Center Valley, PA, USA; IX71). The images were acquired by Photometric CoolSnap HQ camera (Photometric, Tucson, AZ, USA) using $\times 20$ magnification and imported into MetaMorph software (Molecular Device, Sunnyvale, CA, USA). **(d)** The images were enhanced by digital thresholding and the percentage of apoptotic cells was calculated as total area occupied by FITC-stained cells/total area occupied by 4,6-diamidino-2-phenylindole-stained cell for the same image. The bars represent the mean % of apoptotic cells \pm s.d. ($n > 3$).

We have previously demonstrated the ability of BSO to modulate L-PAM resistance in neuroblastoma cell lines established at disease progression including those progressing after myeloablative therapy using L-PAM.^{20,48} We have shown that the optimal activity in multidrug-resistant neuroblastoma

cell lines requires use of L-PAM concentrations only achievable with hematopoietic stem cell support.²⁰ Based on our preclinical data, a phase I study of dose-escalating L-PAM to myeloablative levels when given with BSO and supported by autologous stem cell infusion was recently completed in the NANT consortium

Table 1. Response induced by BSO + L-PAM treatment regimen and its effect on mean RTV, T/C %, median EFS and EFS T/C in MM xenograft models

Groups	N	CR (%)	MCR (%)	PR (%)	PD (%)	Mean RTV mm ³	T/C (RTV) %	Median EFS	EFS T/C
MM.1S									
Control	5	0	0	0	5 (100)	1368.1	100.00	9	1
BSO	5	0	0	0	5 (100)	1573.2	114.99	11	1.2
L-PAM	10	0	0	8 (80)	2 (20)	153.3	11.20	23	2.5
BSO + L-PAM	10	10 (100)	1 (10)	0	0	32.3	2.36	53 ^{a,b,c}	5.8
OPM-2									
Control	5	0	0	0	5 (100)	1308.0	100.00	10	1
BSO	5	0	0	0	5 (100)	1367.0	104.51	13	1.3
L-PAM	5	1 (20)	0	1 (20)	3 (60)	835.5	63.88	18	1.8
BSO + L-PAM	7	7 (100)	5 (71.4)	0	0	412.2	31.51	100 ^{a,b,c}	10
KMS-12-PE									
Control	5	0	0	0	5 (100)	1556.5	100.00	10	1
BSO	5	0	0	0	5 (100)	1557.2	100.04	10	1
L-PAM	6	1 (16.6)	0	0	5 (83.3)	704.8	45.28	17.5	1.7
BSO + L-PAM	8	4 (50)	0	2 (25)	2 (25)	280.9	18.05	44.5 ^{a,b,c}	4.4
All models									
Control	15	0	0	0	15 (100)	1410.9	100.00	10	1
BSO	15	0	0	0	15 (100)	1499.1	106.26	11	1.1
L-PAM	21	2 (9.5)	0	12 (57)	7 (33)	564.5	40.01	20	2
BSO + L-PAM	25	21 (84)	6 (24)	2 (8)	2 (8)	241.8	17.14	53 ^{a,b,c}	5.3

Abbreviations: BSO, buthionine sulfoximine; CR, complete response; EFS, event-free survival; EFS T/C, median EFS of treated group/median EFS of control group; L-PAM, melphalan; MCR, maintained complete response (> 100 days); Mean RTV, mean relative tumor volume on days 8–9; Median EFS, median days taken to reach end point (tumor volume $\geq 1500 \text{ mm}^3$); MM, multiple myeloma; N, total number of mice in a group; PD, progressive disease; PR, partial response; T/C (RTV) %, tumor volume of treated group/tumor volume of control on days 8–9. The table indicates best response induced by vehicle, single agents and combination treatment. ^aRelative to control $P < 0.001$. ^bRelative to BSO $P < 0.001$. ^cRelative to L-PAM $P < 0.001$.

(www.NANT.org; www.clinicaltrials.gov, NCT00005835) and has shown that myeloablative L-PAM given with BSO is well tolerated. As chemotherapy of MM and neuroblastoma both rely heavily on L-PAM and GSH has been shown to enhance L-PAM resistance in MM *in vitro* models,^{8,10} we determined the potential for BSO to enhance L-PAM activity in MM.

We demonstrated that BSO synergistically enhanced L-PAM-induced cytotoxicity for MM *in vitro*. In the majority of cell lines, depletion of GSH by >80% was not cytotoxic, whereas three cell lines were affected by BSO. Our observations are consistent with a previous clinical study in solid tumors where continuous infusion of BSO depleted tumor GSH below 10% of pretreatment levels with minimal systemic toxic effects.^{16,21} L-PAM as a single agent was moderately active in five cell lines and highly active in four cell lines. BSO potentiated the anti-MM activity of L-PAM, inducing >2 logs of cell kill in MM cell lines with a highly aggressive phenotype.^{25,38} As aberrations in the *TP53* gene and t(4:14) translocations are seen in ~15% of patients⁴⁹ and correlated with short progression-free survival and resistance to alkylating agents at relapse,⁵⁰ the ability of BSO to sensitize MM cells with this phenotype suggests that BSO + L-PAM may have clinical activity in the most aggressive forms of MM. Although BSO + L-PAM were not as active in the TX-MM-030h cell line (established at relapse after therapy with myeloablative L-PAM) as in other cell lines, BSO + L-PAM had a greater than additive effect and induced ~3 logs of cell kill. Even in the presence of BMSC and MM cytokines, BSO + L-PAM induced multi-logs of synergistic cytotoxicity (CIN <1.0) and apoptosis ($P < 0.05$) compared with single agents. Similarly, BSO pretreatment synergistically enhanced (CIN <1.0) L-PAM-induced synergistic cytotoxicity in primary MM cells explanted from blood and bone marrows of seven MM patients, six of whom had significant prior exposure to chemotherapy, including myeloablative therapy and SCT.

The potent anti-myeloma activity of BSO + L-PAM that we observed *in vitro* was also observed in MM xenograft mouse

models. The combination treatment, at a non-myeloablative dose, that was maximum tolerated by *beige-nude-xid* mice induced CRs in 100% of the MM.1S and OPM-2 xenografts, while 25% of mice achieved a CR in KMS-12-PE xenografts. One of 10 MM.1S mice and 5/7 OPM-2 mice achieved MCRs. Notably, the combination was highly active against the OPM-2 xenograft model, which has a translocation t(4;14).^{2,50} The doses of BSO (human equivalent dose: 754 mg/m^2)¹² and L-PAM (human equivalent dose: 60 mg/m^2)^{23,51} used in our xenograft studies are lower than the clinically achievable doses in a setting where autologous stem cell support is used. As we have documented the tolerability of L-PAM + BSO when supported by autologous stem cell infusion in heavily pretreated relapsed and/or refractory neuroblastoma patients (NANT phase I study, NCT00005835, www.clinicaltrials.gov), using myeloablative L-PAM + BSO is clinically feasible. The tolerability of myeloablative L-PAM + BSO in our pediatric phase I study taken together with the preclinical data presented here support the feasibility of a phase I trial of L-PAM + BSO in MM.

We showed that BSO alone did not induce apoptosis in MM cell lines. By contrast, BSO significantly enhanced L-PAM-induced apoptosis and cytotoxicity. The effect of BSO-induced GSH depletion is likely by thwarting L-PAM detoxification and therefore increasing L-PAM-induced DNA interstrand crosslinks.^{8–10,13} It is also possible that GSH depletion affects cellular response to DNA damage by partially inhibiting DNA repair because of effects on sulfhydryl-containing repair enzymes and depleting redox environment necessary for repair machinery.^{8,52,53} Both mechanisms of action for BSO could be clinically important because previous studies have demonstrated that increased DNA crosslink/monoadducts and slow repair of DNA damage in L-PAM-treated patients is correlated to longer progression-free survival and improved outcome of treatment.^{13,54}

Our mechanistic investigations demonstrated that BSO + L-PAM induced significant increases in mitochondrial depolarization, cleavage of caspase-3, caspase-9, poly ADP ribose polymerase and DNA fragmentation. Interestingly, BSO

significantly enhanced L-PAM-induced apoptosis in *TP53*-mutated MM cell lines, suggesting that BSO + L-PAM can achieve p53-independent cell death as described previously.^{20,55} As p53 abnormalities are associated with poor prognosis in MM,^{2,49} the ability of BSO + L-PAM to induce cell death by circumventing p53 loss-of-function may provide a viable therapeutic option for patients with del17p13 MM.^{2,49}

L-PAM depleted GSH in the L-PAM-resistant OPM-2 cell line but GSH rapidly recovered. However, BSO treatment of OPM-2 prevented the GSH recovery after L-PAM treatment. A recent report showed that basal GSH levels are significantly elevated in MM patients after receiving therapy, which is consistent with our observation of resistant MM cell lines increasing GSH after L-PAM treatment.⁵⁶ Treatment with thiols (NAC and STS) antagonized the cytotoxic synergy of BSO + L-PAM, mimicking the effect of GSH as previously reported.^{43,57} The effect of NAC is independent of GSH because in the presence of BSO + L-PAM, NAC did not increase GSH levels. Moreover, as non-thiol antioxidants (vitamins C and E) did not antagonize BSO + L-PAM cytotoxicity, it is likely that NAC and STS act to directly replace GSH as an absorbent of the highly reactive L-PAM.

In conclusion, our study demonstrated that depletion of GSH by BSO significantly enhanced the activity of L-PAM against MM *in vitro* and *in vivo*. A recently completed NANT phase I study demonstrated that myeloablative BSO + L-PAM was well tolerated in neuroblastoma patients. Taken together, these data support the development of a phase I clinical trial of BSO + myeloablative dosing of L-PAM and stem cell support in patients with relapsed and refractory MM.

CONFLICT OF INTEREST

The authors declare no conflict of interest.

ACKNOWLEDGEMENTS

We thank Drs Henderson and Fowler for assistance with a cryostat used for sectioning tumors, Janet Derten for assisting with the MetaMorph software, Charlie Linch for assisting with analytical flow cytometry, and Tito Woodburn, Heather Hall and Heather Davidson for assisting with cell culture, STR's and mycoplasma testing. The study was supported in part by National Cancer Institute (NCI) grant CA82830. The TX-MM-030h cell line was provided by the Texas Cancer Cell Repository (www.TXCCR.org) with support from Cancer Prevention & Research Institute of Texas grant RP110763. Clinical grade BSO was provided via an NCI Rapid Access to Intervention Discovery (RAID) grant to CPR.

AUTHOR CONTRIBUTIONS

AT and CPR designed the research and analyzed the data. AT wrote the manuscript and CPR edited the manuscript. HS and MHK analyzed the GSH samples.

REFERENCES

- Dimopoulos MA, San-Miguel JF, Anderson KC. Emerging therapies for the treatment of relapsed or refractory multiple myeloma. *Eur J Haematol* 2011; **86**: 1–15.
- Palumbo A, Anderson K. Multiple myeloma. *N Engl J Med* 2011; **364**: 1046–1060.
- Becker N. Epidemiology of multiple myeloma. *Recent Results Cancer Res* 2011; **183**: 25–35.
- Fernandez de Larrea C, Jimenez R, Rosinol L, Gine E, Tovar N, Cibeira MT et al. Pattern of relapse and progression after autologous SCT as upfront treatment for multiple myeloma. *Bone Marrow Transplant* 2013; **49**: 223–227.
- Lonial S. Relapsed multiple myeloma. *ASH Educ Program Book* 2010; **2010**: 303–309.
- Richardson P, Mitsiades C, Schlossman R, Ghobrial I, Hideshima T, Chauhan D et al. The treatment of relapsed and refractory multiple myeloma. *Hematol Am Soc Hematol Educ Program* 2007; 317–323.
- Kumar SK, Lee JH, Lahuerta JJ, Morgan G, Richardson PG, Crowley J et al. Risk of progression and survival in multiple myeloma relapsing after therapy with IMiDs and bortezomib: a multicenter international myeloma working group study. *Leukemia* 2012; **26**: 149–157.

- Bellamy WT, Dalton WS, Gleason MC, Grogan TM, Trent JM. Development and characterization of a melphalan-resistant human multiple myeloma cell line. *Cancer Res* 1991; **51**: 995–1002.
- Hall AG, Tilley MJ. Mechanisms of action of, and modes of resistance to, alkylating agents used in the treatment of haematological malignancies. *Blood Rev* 1992; **6**: 163–173.
- Mulcahy RT, Bailey HH, Gipp JJ. Up-regulation of gamma-glutamylcysteine synthetase activity in melphalan-resistant human multiple myeloma cells expressing increased glutathione levels. *Cancer Chemother Pharmacol* 1994; **34**: 67–71.
- Mulcahy RT, Bailey HH, Gipp JJ. Transfection of complementary DNAs for the heavy and light subunits of human gamma-glutamylcysteine synthetase results in an elevation of intracellular glutathione and resistance to melphalan. *Cancer Res* 1995; **55**: 4771–4775.
- Bailey HH, L-S, R-buthionine sulfoximine: historical development and clinical issues. *Chem Biol Interact* 1998; **111–112**: 239–254.
- Dimopoulos MA, Souliotis VL, Anagnostopoulos A, Bamia C, Pouli A, Baltadakis I et al. Melphalan-induced DNA damage in vitro as a predictor for clinical outcome in multiple myeloma. *Haematologica* 2007; **92**: 1505–1512.
- Griffith OW, Meister A. Potent and specific inhibition of glutathione synthesis by buthionine sulfoximine (S-n-butyl homocysteine sulfoximine). *J Biol Chem* 1979; **254**: 7558–7560.
- Griffith OW. Mechanism of action, metabolism, and toxicity of buthionine sulfoximine and its higher homologs, potent inhibitors of glutathione synthesis. *J Biol Chem* 1982; **257**: 13704–13712.
- O'Dwyer PJ, Hamilton TC, LaCreta FP, Gallo JM, Kilpatrick D, Halbherr T et al. Phase I trial of buthionine sulfoximine in combination with melphalan in patients with cancer. *J Clin Oncol* 1996; **14**: 249–256.
- Dorr RT, Liddil JD, Soble MJ. Cytotoxic effects of glutathione synthesis inhibition by L-buthionine-(SR)-sulfoximine on human and murine tumor cells. *Invest New Drugs* 1986; **4**: 305–313.
- Bailey HH, Mulcahy RT, Tutsch KD, Arzooarian RZ, Alberti D, Tombes MB et al. Phase I clinical trial of intravenous L-buthionine sulfoximine and melphalan: an attempt at modulation of glutathione. *J Clin Oncol* 1994; **12**: 194–205.
- Anderson CP, Tsai JM, Meek WE, Liu RM, Tang Y, Forman HJ et al. Depletion of glutathione by buthionine sulfoximine is cytotoxic for human neuroblastoma cell lines via apoptosis. *Exp Cell Res* 1999; **246**: 183–192.
- Anderson CP, Reynolds CP. Synergistic cytotoxicity of buthionine sulfoximine (BSO) and intensive melphalan (L-PAM) for neuroblastoma cell lines established at relapse after myeloablative therapy. *Bone Marrow Transplant* 2002; **30**: 135–140.
- Bailey HH, Ripple G, Tutsch KD, Arzooarian RZ, Alberti D, Feierabend C et al. Phase I study of continuous-infusion L-S-R-buthionine sulfoximine with intravenous melphalan. *J Natl Cancer Inst* 1997; **89**: 1789–1796.
- Smith AC, Liao JT, Page JG, Wientjes MG, Grieshaber CK. Pharmacokinetics of buthionine sulfoximine (NSC 326231) and its effect on melphalan-induced toxicity in mice. *Cancer Res* 1989; **49**: 5385–5391.
- Grigoryan RS, Yang B, Keshelava N, Barnhart JR, Reynolds CP. Flow cytometry analysis of single-strand DNA damage in neuroblastoma cell lines using the F7-26 monoclonal antibody. *Cytometry A* 2007; **71**: 951–960.
- Kang MH, Kang YH, Szymanska B, Wilczynska-Kalak U, Sheard MA, Hamed TM et al. Activity of vincristine, L-ASP, and dexamethasone against acute lymphoblastic leukemia is enhanced by the BH3-mimetic ABT-737 in vitro and in vivo. *Blood* 2007; **110**: 2057–2066.
- Drexler HG, Matsuo Y. Malignant hematopoietic cell lines: in vitro models for the study of multiple myeloma and plasma cell leukemia. *Leuk Res* 2000; **24**: 681–703.
- Grigoryan R, Keshelava N, Anderson C, Reynolds CP. In vitro testing of chemosensitivity in physiological hypoxia. *Methods Mol Med* 2005; **110**: 87–100.
- Chatterjee M, Honemann D, Lentzsch S, Bommert K, Sers C, Herrmann P et al. In the presence of bone marrow stromal cells human multiple myeloma cells become independent of the IL-6/gp130/STAT3 pathway. *Blood* 2002; **100**: 3311–3318.
- Zlei M, Egert S, Wider D, Ihorst G, Wasch R, Engelhardt M. Characterization of in vitro growth of multiple myeloma cells. *Exp Hematol* 2007; **35**: 1550–1561.
- Keshelava N, Frgala T, Krejsa J, Kalous O, Reynolds CP. DIMSCAN: a microcomputer fluorescence-based cytotoxicity assay for preclinical testing of combination chemotherapy. *Methods Mol Med* 2005; **110**: 139–153.
- Frgala T, Kalous O, Proffitt RT, Reynolds CP. A fluorescence microplate cytotoxicity assay with a 4-log dynamic range that identifies synergistic drug combinations. *Mol Cancer Ther* 2007; **6**: 886–897.
- Kang MH, Smith MA, Morton CL, Keshelava N, Houghton PJ, Reynolds CP. National Cancer Institute pediatric preclinical testing program: model description for in vitro cytotoxicity testing. *Pediatr Blood Cancer* 2011; **56**: 239–249.
- Pinguet F, Martel P, Fabbro M, Petit I, Canal P, Culine S et al. Pharmacokinetics of high-dose intravenous melphalan in patients undergoing peripheral blood hematopoietic progenitor-cell transplantation. *Anticancer Res* 1997; **17**: 605–611.

- 33 Falco P, Brinthen S, Avonto I, Gay F, Morabito F, Boccadoro M *et al*. Melphalan and its role in the management of patients with multiple myeloma. *Expert Rev Anticancer Ther* 2007; **7**: 945–957.
- 34 Paroni R, De Vecchi E, Cighetti G, Arcelloni C, Fermo I, Grossi A *et al*. HPLC with o-phthalaldehyde precolumn derivatization to measure total, oxidized, and protein-bound glutathione in blood, plasma, and tissue. *Clin Chem* 1995; **41**: 448–454.
- 35 Tomayko MM, Reynolds CP. Determination of subcutaneous tumor size in athymic (nude) mice. *Cancer Chemother Pharmacol* 1989; **24**: 148–154.
- 36 Reynolds CP, Sun BC, DeClerck YA, Moats RA. Assessing growth and response to therapy in murine tumor models. *Methods Mol Med* 2005; **111**: 335–350.
- 37 Houghton PJ, Morton CL, Tucker C, Payne D, Favours E, Cole C *et al*. The pediatric preclinical testing program: description of models and early testing results. *Pediatr Blood Cancer* 2007; **49**: 928–940.
- 38 Chauhan D, Tian Z, Zhou B, Kuhn D, Orlowski R, Raje N *et al*. *In vitro* and *in vivo* selective antitumor activity of a novel orally bioavailable proteasome inhibitor MLN9708 against multiple myeloma cells. *Clin Cancer Res* 2011; **17**: 5311–5321.
- 39 Matsuo Y, Nakamura S, Adachi T, Tsubota T. Establishment and characterization of new IgD lambda type myeloma cell lines, MOLP-2 and MOLP-3, expressing CD28, CD33 antigens and the IL-6 receptor. *Hum Cell* 1993; **6**: 310–313.
- 40 Corradini P, Inghirami G, Astolfi M, Ladetto M, Voena C, Ballerini P *et al*. Inactivation of tumor suppressor genes, p53 and Rb1, in plasma cell dyscrasias. *Leukemia* 1994; **8**: 758–767.
- 41 Taylor RC, Cullen SP, Martin SJ. Apoptosis: controlled demolition at the cellular level. *Nat Rev Mol Cell Biol* 2008; **9**: 231–241.
- 42 Kepp O, Galluzzi L, Lipinski M, Yuan J, Kroemer G. Cell death assays for drug discovery. *Nat Rev Drug Discov* 2011; **10**: 221–237.
- 43 Muldoon LL, Walker-Rosenfeld SL, Hale C, Purcell SE, Bennett LC, Neuwelt EA. Rescue from enhanced alkylator-induced cell death with low molecular weight sulfur-containing chemoprotectants. *J Pharmacol Exp Ther* 2001; **296**: 797–805.
- 44 Rajkumar SV. Treatment of multiple myeloma. *Nat Rev Clin Oncol* 2011; **8**: 479–491.
- 45 Kumar SK, Therneau TM, Gertz MA, Lacy MQ, Dispenzieri A, Rajkumar SV *et al*. Clinical course of patients with relapsed multiple myeloma. *Mayo Clin Proc* 2004; **79**: 867–874.
- 46 van de Donk NW, Lokhorst HM, Dimopoulos M, Cavo M, Morgan G, Einsele H *et al*. Treatment of relapsed and refractory multiple myeloma in the era of novel agents. *Cancer Treat Rev* 2011; **37**: 266–283.
- 47 Lee HC, Shah JJ, Orlowski RZ. Novel approaches to treatment of double-refractory multiple myeloma. *Am Soc Clin Oncol Educ Book* 2013; **2013**: 302–306.
- 48 Anderson CP, Tsai J, Chan W, Park CK, Tian L, Lui RM *et al*. Buthionine sulfoximine alone and in combination with melphalan (L-PAM) is highly cytotoxic for human neuroblastoma cell lines. *Eur J Cancer* 1997; **33**: 2016–2019.
- 49 Munshi NC, Avet-Loiseau H. Genomics in multiple myeloma. *Clin Cancer Res* 2011; **17**: 1234–1242.
- 50 Jaksic W, Trudel S, Chang H, Trieu Y, Qi X, Mikhael J *et al*. Clinical outcomes in t(4;14) multiple myeloma: a chemotherapy-sensitive disease characterized by rapid relapse and alkylating agent resistance. *J Clin Oncol* 2005; **23**: 7069–7073.
- 51 Palumbo A, Brinthen S, Bruno B, Falcone AP, Liberati AM, Grasso M *et al*. Melphalan 200 mg/m² versus melphalan 100 mg/m² in newly diagnosed myeloma patients: a prospective, multicenter phase 3 study. *Blood* 2010; **115**: 1873–1879.
- 52 Révész L, Edgren M. Glutathione-dependent yield and repair of single-strand DNA breaks in irradiated cells. *Br J Cancer Suppl* 1984; **6**: 55–60.
- 53 Oleinick NL, Xue LY, Friedman LR, Donahue LL, Biaglow JE. Inhibition of radiation-induced DNA-protein cross-link repair by glutathione depletion with L-buthionine sulfoximine. *NCI Monogr* 1988; **6**: 225–229.
- 54 Dimopoulos MA, Souliotis VL, Anagnostopoulos A, Papadimitriou C, Sfikakis PP. Extent of damage and repair in the p53 tumor-suppressor gene after treatment of myeloma patients with high-dose melphalan and autologous blood stem-cell transplantation is individualized and may predict clinical outcome. *J Clin Oncol* 2005; **23**: 4381–4389.
- 55 Strasser A, Harris AW, Jacks T, Cory S. DNA damage can induce apoptosis in proliferating lymphoid cells via p53-independent mechanisms inhibitable by Bcl-2. *Cell* 1994; **79**: 329–339.
- 56 Mehdi WA, Zainulabdeen JA, Mehde AA. Investigation of the antioxidant status in multiple myeloma patients: effects of therapy. *Asian Pac J Cancer Prev* 2013; **14**: 3663–3667.
- 57 Zhang F, Lau SS, Monks TJ. The cytoprotective effect of N-acetyl-L-cysteine against ROS-induced cytotoxicity is independent of its ability to enhance glutathione synthesis. *Toxicol Sci* 2011; **120**: 87–97.



This work is licensed under a Creative Commons Attribution-NonCommercial-NoDerivs 3.0 Unported License. The images or other third party material in this article are included in the article's Creative Commons license, unless indicated otherwise in the credit line; if the material is not included under the Creative Commons license, users will need to obtain permission from the license holder to reproduce the material. To view a copy of this license, visit <http://creativecommons.org/licenses/by-nc-nd/3.0/>

Supplementary Information accompanies this paper on Blood Cancer Journal website (<http://www.nature.com/bcj>)